Desalination and Water Treatment
www.deswater.com

doi: 10.5004/dwt.2019.23393

142 (2019) 213–224
February

Synthesis and characterization of immobilized 1-(1,3-diphenyl-5-hydroxy-1*H*-pyrazol-4-yl)ethanone on silica gel and its use for aqueous heavy metal removal

Farah Suhail[a], Madeeha Batool[a,*], Muhammad Imran Din[a], Misbahul Ain Khan[a,b], Khurshid Ayub[c], Sobia Tabassum[d], Asma Tufail Shah[d]

[a]*Institute of Chemistry, University of the Punjab, Lahore 54590, Pakistan, Tel. +92-042-99230463 Ext. 813; emails: s_madeeha_b@yahoo.com (M. Batool), fast.780@gmail.com (F. Suhail), imrandin2007@gmail.com (M.I. Din)*
[b]*Department of Chemistry, The Islamia University of Bahawalpur, Bahawalpur, PK 63100, Pakistan, email: misbahakhan@gmail.com*
[c]*Department of Chemistry, COMSATS Institute of Information Technology, Abbottabad Campus 22060, Pakistan, email: khurshid@ciit.net.pk*
[d]*Interdisciplinary Research Centre in Biomedical Materials (IRCBM), COMSATS Institute of Information Technology, Lahore 54600, Pakistan, email: sobiatabassum@cuilahore.edu.pk (S. Tabassum), drasmashah@cuilahore.edu.pk (A.T. Shah)*

Received 26 April 2018; Accepted 30 October 2018

ABSTRACT

A novel, alternative and efficient organic-inorganic hybrid was synthesized by immobilizing 1-(1,3-diphenyl-5-hydroxy-1*H*-pyrazol-4-yl)ethanone on silica gel, previously modified with 3-aminopropyltrimethoxysilane. This novel material was well characterized by fourier transform infrared spectroscopy, ^{29}Si and ^{13}C cross-polarization magic-angle-spinning solid-state nuclear magnetic resonance, scanning electron microscopy, Brunauer–Emmett–Teller surface area, X-ray diffraction and elemental analysis. Thermal stability of the material was determined by thermogravimetry curves (TGA). This new chelating agent effectively removed Lead ions Pb(II) from the aqueous solution and showed very high adsorption capacity (q_e (mg/g) up to 120.83 mg/g for hyper toxic Pb(II) ions.

Keywords: Modified silica gel; Pyrazolone; Adsorption; Pb(II); Kinetics; Thermodynamics; Isotherms

1. Introduction

Heavy metals like lead, chromium, arsenic, mercury etc in wastewater of industries cause significant toxic effects to the environment. If the concentration of heavy metals exceeds from a certain safe and allowable limit, it can cause health issues to both human and aquatic life. Lead is a non biodegradable element and accumulates in living organisms. Even, low concentration of lead can cause different diseases and disorders [1–4]. Over the years, various methods which include adsorption, ion exchange, solvent extraction, coagulation [5], membrane separation, reverse osmosis, cementation and chemical precipitation [6] have been developed for heavy metal removal from waste water.

For adsorption, different types of adsorbents e.g. zeolites, activated carbon, clay, peat, fly ash etc. are used. Most of these adsorbents have low thermal and mechanical stability, low bond strength, high cost and poor removal of metal ions. To overcome these problems, organic-inorganic hybrid materials based on silica sources have been used. Porous polysiloxanes SiO_2 (silica) is an adsorbent but when modified with selected organic groups, gains renewed interest. Major advantages of using silica gel as a support include its high mechanical and thermal stability, high surface area [7] and easy modification of surface silanol groups [8] with some organic moiety to make organo-fuctionalized silanes. Although, no specific interaction with metal ions is shown by unmodified porous

---

* Corresponding author.

silica, but when organic moiety is attached to it, metal ion complexation property is enhanced to a significant extent [9]. Donoratoms (for example O, S and N) of organic molecules immobilized on the surface of silica can make complexes with a number of metal ions and show their selective and distinguishable extraction properties [10].

Pyrazole unit is a part of many natural products. Like other nitrogen-containing heterocycles [11,12], it has good capability of coordinating with metal ions. Its *sp*^{2} hybrid nitrogen donors make its derivatives a good ligand [13–15].A number of articles are available in which derivatives of pyrazole have been covalently immobilized to the surface of modified silica through Schiff base formation that facilitates the immobilization of organic moiety on silica surface. Because of β-diketone system in 4-acylpyrazolone ligand, it has been used as organic part of different hybrids. Different metals like Pr(III), Eu(III), Tb(III) and Yb(III) have been separated by 4-benzoyl and 4-capryloyl derivatives of 5-pyrazolone [16].

SmaailRadi and his co-workers have contributed a lot in the removal of heavy metals using a number of silica-supported pyrazoleadsorbents. They reported hydroxybipyrazole [17], bipyrazoltripodal [18], bis(3,5-dimethylpyrazole [19], acyclic pyrazole [20] derivatives, pyridylpyrazole derivative [9], 1,5-dimethylpyrazole-3-carbaldehyde [10] and 3-methyl-1-phenylpyrazolone [21] anchored on modified silica surface and studied their adsorption properties. Highly selective and efficient adsorption of Hg was reported using hydroxyethyl derivative of pyrazole [22]. Cu(II) metal was selectively adsorbed [23] by modifying the surface of silica with 3,5-dimethylpyrazole. Tetrapyrazole [24] functionalized silica gel and Merrifield resin were used for extraction of metals from aqueous solution. Adsorption properties of lanthanide ions (selectively of Yb(III)) [25] were also studied using derivative of pyrazole on modified TEOS. Ion imprinting technique was used for selective adsorption of Th(IV) [26] by silica-supported pyrazole derivative. Solid phase extraction technique (SPE) is efficiently involved in separation/pre-concentration of heavy metals using different inorganic and organic moieties [27–32]. Major advantages of SPE technique include environmental friendliness, high selectivity, flexibility, higher enrichment factors, safety in case of hazardous samples, simple operation, lower cost and less time, lower consumption of reagents, and can easily be combined with different modern detection techniques [33].

In continuation of the research on immobilization of pyrazole derivative on silica surface, we report a novel, efficient and highly selective material (SP) for the removal of Pb(II) ions from aqueous solution. Our adsorbent shows very high value of adsorption capacity (q_e in mg/g) for Pb(II) ions than the reported literature. All the parameters and models upon which adsorption capacity depends have also been studied in detail.

2. Experimental

2.1. Material and Instruments

The solvents and chemicals of usual analytical grade were used with no further purification. Activated silica gel (heated at 160°C for 24 h) with 70–230 mesh particle size and 60 Å median pore diameter, was used. 3-Aminopropyltriethoxysilane (APTES) was used as silylating agent. Flame atomic absorption spectrophotometer of Perkin Elmer, A Analyst 100 was used for measuring metal ions. The pH value was controlled by a digital pH-meter (HANNA, Model-8417). Fourier transform infrared (FTIR) spectra were recorded using Agilent technology model 41630. The solid state ^{29}Si and ^{13}C nuclear magnetic resonance (NMR) were obtained by Bruker AV II 400WB 100 MHz instrument. SEM image were obtained on TESCAN Vega3 LMU Scanning electron microscope (SEM). The thermogravimetric analysis was performed by Perkin Elmer Diamond TG/DTA at a heating rate of 10°C min^{-1} in 90:10 oxygen/nitrogen atmospheres. The Brunauer–Emmett–Teller (BET) specific surface area and other surface properties of the new material were determined by nitrogen gas adsorption/desorption technique. X-ray diffraction spectra were obtained by X-ray diffractometer (XRD), PANalytical XPERT-PRO model. For elemental analysis LECO CHN 628 was used.

2.2. Preparation of pyrazole modified silica

2.2.1. Synthesis of 1-(1,3-diphenyl-5-hydroxy-1H-pyrazol-4-yl) ethanone(**1**)

1,3-Diphenyl-4,5-dihydro-1*H*-pyrazol-5-one was synthesized by the literature available method [34] using phenyl hydrazine and ethyl benzoylacetate (yield = 79%, M.p. = 138°C–139°C). infrared (cm^{-1}):1,700 (lactone C=0), 1,592 and 1,499 (phenyl). Acylation of this product was done by using acetyl chloride as reported by Jensen [35] to get 1-(1,3-diphenyl-5-hydoxy-1*H*-pyrazol-4-yl)ethanone**(1)**. (yield = 85%, M.p = 145°C). IR (cm^{-1}): 1,458 and 1,492 phenyl ring, 1619 (acyl > C=O), 2,600 (intramolecular hydrogen bonding (O–H…O) 3,100-3,200 (intermolecular H-bonding).

2.2.2. Synthesis of amine-modified silica (SN) (**2**)

25 g of Silica gel (activated SiO_2)and 10 mL of aminopropyltriethoxysilane (APTES) was refluxed in dry toluene (150 mL) under inert nitrogen environment to get the product 3-aminopropylsilica (SN) (**2**) as available in literature [10], followed by Soxhlet extraction using ethanol and dichloromethane (1:1 mixture) for 24 h.

2.2.3. Synthesis of ((1,3-diphenyl-5-hydroxy-1H-pyrazol-4-yl) ethanimidoyl-substituted silica (SP) (**3**)

To obtain the Schiff base of 1-(1,3-diphenyl-5-hydroxy-1*H*-pyrazol-4-yl)ethanone, pyrazole derivative (**1**) (1g) and 3-aminopropylsilica (SN) (**2**) (1.66g) were refluxed in dry ethanol for 8 h and then Soxhlet extracted the dried product (modified silica SP (**3**)) in acetonitrile, methanol and dichloromethane for 24 h respectively [10].

2.3. Batch experiment

50 mL of 50 mg/L solution of Pb(II) ions was shaken with 20 mg of the adsorbent (SP) (**3**) under various p*H* conditions (5–7) at 20°C to 50°C for 0 to 120 min at 150 rpm. The solutions were left for 10 min before filtration, followed by metal ion determination by atomic absorption spectrophotometer.

Sorption capacity (q_e, mg/g) of adsorbent and percentage removal (% R) of metal were measured by using the following equations:

$$q_e = \frac{(C_o - C_e)}{m} \times V \tag{1}$$

$$\%R = \frac{(C_o - C_e)}{C_o} \times 100 \tag{2}$$

where C_o (mg/L) is initial concentration of metal ion, C_e (mg/L) is equilibrium metal ion concentration, m (g) is the mass of adsorbent and V (L) is the volume of the metal solution used for the experiment.

2.4. Computational method

All calculations have been executed by using Gaussian 09 suit of programs [36]. The geometry of SP material has been optimized at B3LYP/6-31G (d, p) level of theory. Frequency calculation has been carried out at the same level to ascertain that the optimized geometry of SP belongs to true minimum (absence of any imaginary frequency).

3. Result and Discussion

The scheme for the synthesis of new adsorbent is shown in Fig. 1. The ligand was prepared by acylation of the pyrazole derivative using acetyl chloride. The structure of synthesized ligand was confirmed by spectroscopic methods. Activated silica gel was functionalized with 3-aminopropyltriethoxysilane (APTES) in toluene to attach amino group (–NH_2) to the surface of silica. Both reactants were mixed and refluxed in dry ethanol to form new chelating agent (SP) (Fig. 1). NH_2^- group of silica and acyl group of pyrazole derivative reacted to form Schiff base in adsorbent SP.

3.1. Characterizations

3.1.1. Fourier transform infrared

FTIR spectra of silica gel (SG), 3-aminopropylsilica (SNH) and pyrazole modified silica (SP) is shown in Fig. 2. A prominent sharp peak at 1056 cm^{-1} was observed in free silica spectra attributed to Si–O–Si stretching vibrations. A shoulder peak at 976 cm^{-1} corresponded to Si–O vibration. A broad band of O–H vibration was present around 3000–3600 cm^{-1} [37].Comparing with free silica, spectrum of aminopropylsilica (SN) was distinguished by the appearance of NH_2 and CH_2 vibration at 1556 $cm^{-1}$and 2928 cm^{-1} respectively [38]. The disappearance of primary amine (NH_2) peak at 1556 cm^{-1} and the appearance of a new peak of C=N vibrations at 1507 cm^{-1} in the FTIR spectrum of SP confirmed the immobilization of pyrazole derivative onto silica surface [10].

FTIR of silica supported pyrazole derivative has also been calculated theoretically. The theoretically calculated spectrum contains all major peaks as discussed for the experimental FTIR spectrum (Fig. S1).

3.1.2. NMR characterization

Solid state NMR gives qualitative information about the nature of atom present in molecule. No quantitative information is easy to obtain as peak intensity in NMR is difficult to correlate with the concentration of attached species on surface. The ^{29}Si NMR spectrum gives qualitative information about the nature and coordination of silicon atom, either present in silane chain or in silica gel. The solid state ^{29}Si NMR spectrum of the pyrazole functionalized silica adsorbent (SP) is shown in Fig. 3(a). Two prominent peaks appeared in the spectrum; one at –67.54 ppm and the other at –110.46 ppm with a shoulder peak at –101.26 ppm. The peak at –67.54 ppm belonged to silicon atom of attached APTES, which bound to the surface of silica in bidentate binding mode (–Si–(OEt)(O–Si)$_2$–CH_2–) with a free ethoxy group [39].

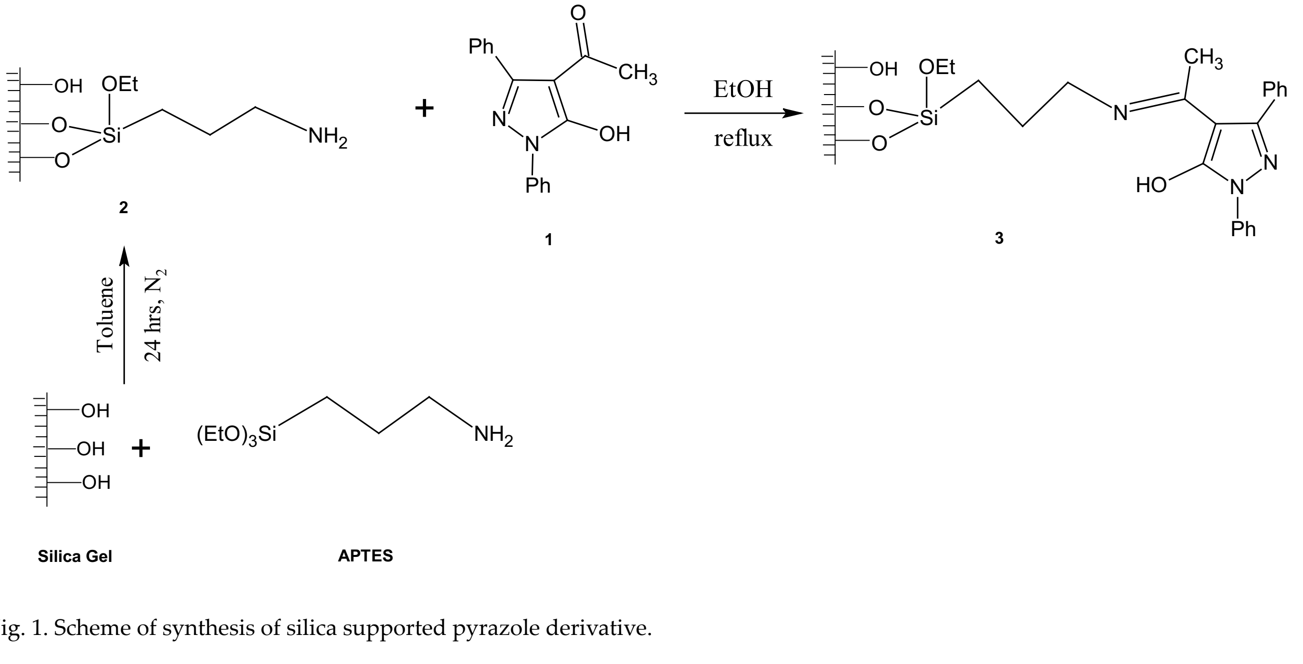

Fig. 1. Scheme of synthesis of silica supported pyrazole derivative.

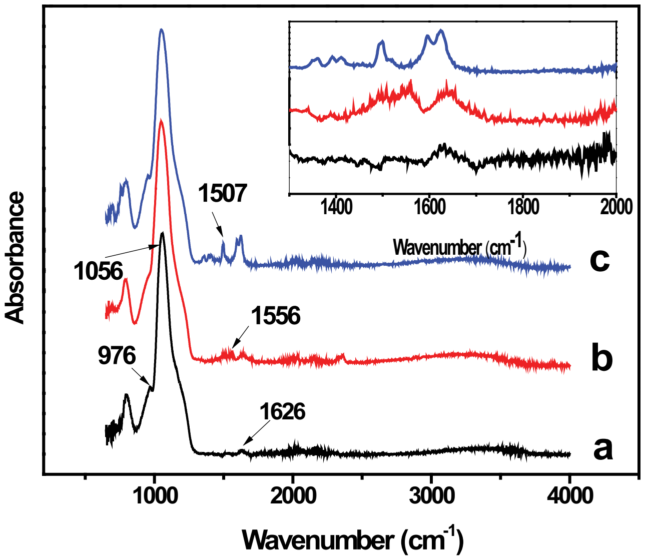

Fig. 2. FTIR spectra of (a) silica gel (SG), (b) 3-aminopropylsilica (SNH) and(c) SP.

The second peak at –110.46 ppm corresponded to the silicon atom of silica gel attached to four other silicon atoms through oxygen atom (–Si(OSi–)$_4$–). The shoulder peak at –101.26 ppm corresponded to a Q^3 species of silica gel silicon atom (–Si(OH)(OSi–)$_3$–) which was attached to one hydroxyl group and three silicon atoms through oxygen atom [25,40] representing surface silica atoms.

The occurrence of reaction between silica surface and APTES to form SN and then the reaction between amino group of SN and carbonyl derivative of pyrazole to form final product SP was easily verified by taking solid state ^{13}C NMR spectrum of SP adsorbent (Fig. 3(b)). The signal at 172.29 ppm attributed to imine carbon (C=N). The weak signals at167.98, 164.79 and 61.52 ppm assigned to C-5, C-3 and C-4 of pyrazole ring, respectively. The ethoxy carbon (–OCH$_2$CH$_3$) has been observed by a peak at 45.28 ppm while the methylene group attached to nitrogen (–CH$_2$N=) was shown by the signal at 41.72 ppm. A sharp peak at 20.67 ppm was observed for methylene group (–CH$_2$CH$_2$N=). Two methyl groups (–CH$_3$) have shown weak signals at 16.42 and 15.38 ppm. Another sharp peak at 8.68 ppm was observed due to –CH$_2$Si. The remaining signals were for phenyl ring carbons: C-1′ (139.06 ppm) phenyl carbon attached with nitrogen of pyrazole ring, C-1″ (137.86 ppm) phenyl carbon attached with carbon of pyrazole ring, C-2′, C-6′ (118.07 ppm), C-2″, C-6″, C-4′, C-4″ (127.74 ppm) and C-3′, C-5′, C-3″, C-5″ (134.33 ppm).

Absence of signal *ca.* δ = 200 ppm for carbonyl carbon if attached to pyrazole at C4 position and appearance of characteristic peak of imine (C=N) at 172.29 ppm has confirmed the successful reaction between amino group of SN and carbonyl carbon of pyrazole derivative to yield Schiff's base. Appearance of signal at 45.28 ppm indicated the presence of one free alkoxy group on silicon which bound to silica surface in bindentate mode.

3.1.3. Scanning electron microscope

The morphology and structure of the novel adsorbent (SP) was examined by taking scanning electron micrographs (SEM) at 100× and 500× magnifications (Fig. 4). The smooth surface of unmodified silica gel turned in to a rough surface after modification. Both the whole rough surface and un-agglomeration of silica surface after modification with pyrazole supported the claim of regular distribution of organic moiety upon the silica surface reported earlier [10].

3.1.4. Elemental analysis

The activated silica gel did not contain any carbon or nitrogen content. The carbon, hydrogen and nitrogen content found in novel adsorbent SP were 7.05%, 6.44% and 3.62% respectively. The occurrence of carbon and nitrogen content in synthesized adsorbent indicated the successful immobilization of the required organic moiety. Total content of carbon and nitrogen (10.67%) in adsorbent SP corresponded to the 348 µmol/g of carbon and nitrogen organic moiety attached to the silica surface.

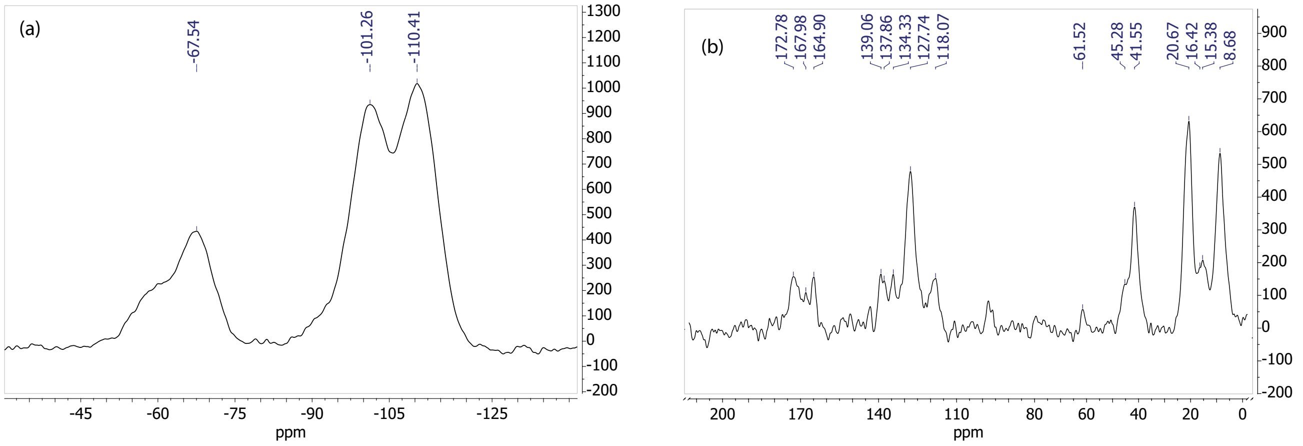

Fig. 3. (a) ^{29}Si NMR spectra of SP (b) ^{13}C NMR spectra of SP.

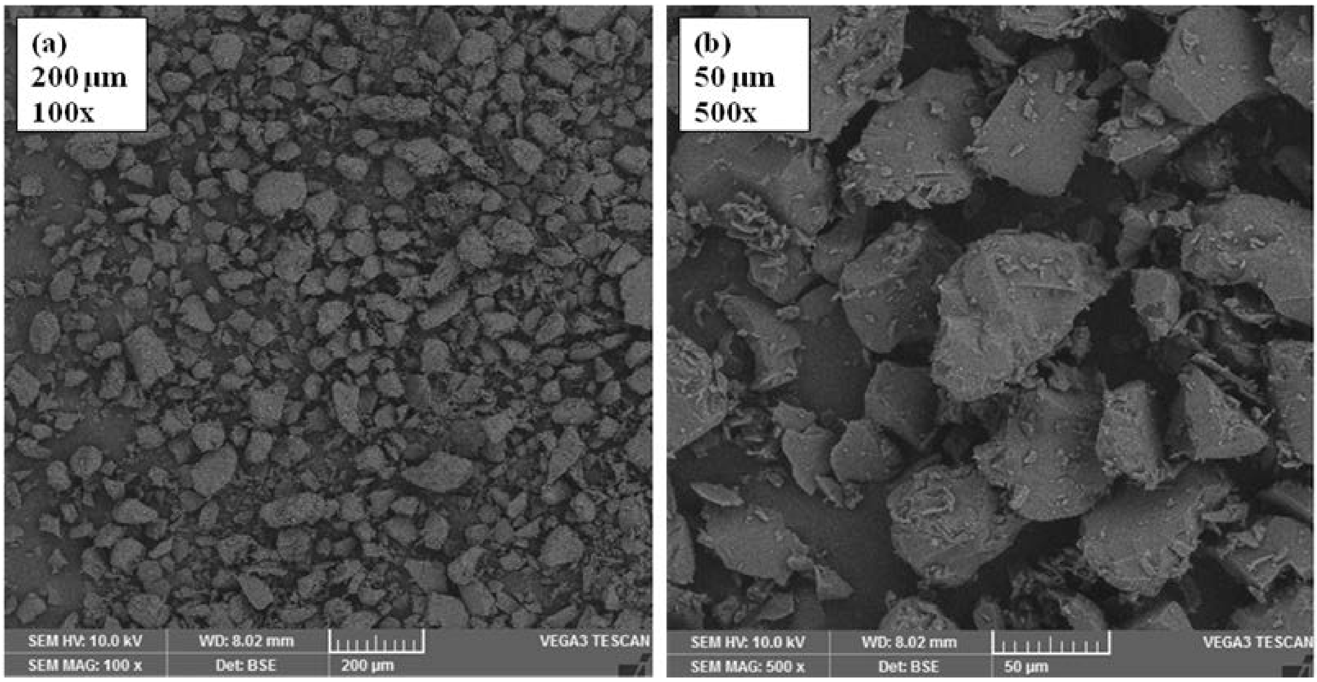

Fig. 4. SEM images of SP at different magnification (a) 200 µm, 100× and (b) 50 µm, 500×.

3.1.5. TGA analysis

The thermo gravimetric analysis of unmodified (SG), amine-modfied (SN) and pyrazole-modified (SP) gives the information about the thermal stability of the compounds and also confirmed the amount of organic compound immobilized on the surface. The curve (Fig. 5) showed high thermal stability of the material as degradation process occurred at 150°C–800°C. In the TGA curve of silica gel, first weight loss of 10.5% up to temperature 150°C was assigned to the removal of physically adsorbed water. The next weight loss of 2.49% up to 800°C was attributed to the formation of siloxane bond after condensation of free silanol groups [41]. In case of SN, weight loss also occurred in two steps; the weight loss of 9.87% from room temperature to 150°C appeared in the first step and the weight loss of 9.75% between the temperatures 150°C to 800°C appeared in the second step, which was assigned to the remaining silanol hydration water and the attached amine group decomposition respectively. The decomposition of amine group above 150°C indicated its attachment through chemical bond. Similarly in case of SP the weight loss of 5.57% up to 118°C was because of adsorbed water and a weight loss of 13.88% from 150°C to 800°C was evident of decomposition of immobilized pyrazole and remaining organic fraction. The high value of weight loss in the second step indicated the higher amount of immobilized organic molecule. The mass lost in second step (13.88%) can be used to calculate the amount of organic moiety immobilized on silica surface of SP corresponding to the molecular mass of the relevant carbon chain. Hence, the amount of organic part attached to silica surface was calculated to be 382 µmolg^{-1} which was in agreement with the elemental analysis results.

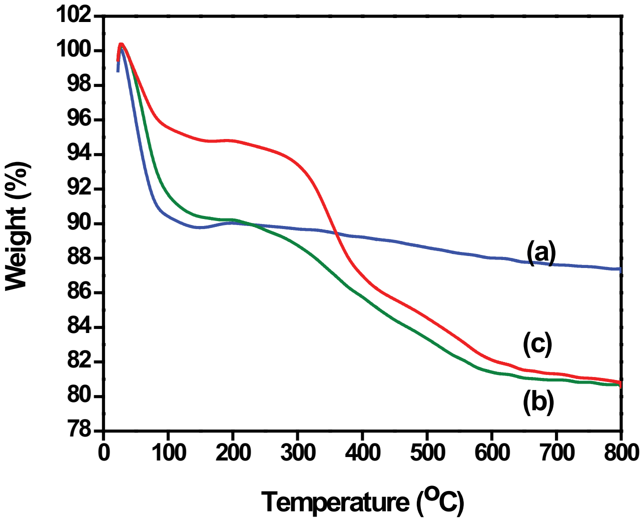

Fig. 5. TGA of SG (a), SN (b) and SP (c).

3.1.6. Surface properties

The surface properties of inorganic silica backbone were changed due to covalent attachment of pyrazole derivative. The initial specific surface area of silica gel was 305.21 m^{2}g^{-1} and pore volume was 0.77 cm^{3}g^{-1} (Table 1). The immobilization of pyrazole derivative caused the decrease in the specific surface area as well asin the pore volume to198.98 m^{2}g^{-1} and 0.27 cm^{3}g^{-1} respectively. The bigger organic moieties grafted on the silica surface occupied the space around the pores to partially block them, resulting in less approach of nitrogen atoms to the silica surface [10].

Table 1
Surface properties of pyrazole-modified silica

Silica derivative	Specific surface S_{BET} (m^2/g)	Pore volume (cm^3/g)
SG	305.21	0.77
SP	198.98	0.27

3.1.7. X-Ray diffraction

The XRD patterns of unmodified and modified silica (Fig. 6) indicated that amorphous structure of silica retained even after grafting of the organic part. All diffractro grams exhibited a characteristic broad peak at high 2θ angle range (i.e. 22°) for a typical amorphous silica halo [42]. A decrease in peak intensity of the grafted material was clearly observed while comparing with the unmodified silica as reported in literature [43] of similar silica hybrid.

3.2. Density functional theory calculations

The first step towards optimization of silica supported pyrazole derivative (SP) is the selection of silicon-oxygen ring network to model the silica surface. Hydroxy groups have been inserted for termination. After designing the silica surface, APTES and pyrazole derivatives have been added and the resultant structure has been optimized as shown in Fig. 7. From the optimized geometry, some prominent structural features can be tracked like the pyrazole ring, *N*-phenyl ring and imine moiety are co-planar. The second phenyl group is deviated from the plane of pyrazole ring.

Frontier molecular orbital (FMO) analysis has been performed to gain an insight into the mechanism of adsorption of Pb(II) by the SP. The HOMO is mainly distributed over the pyrazole ring and imine moiety whereas LUMO is dispersed over the phenyl ring (Fig. 8). The density of HOMO over imine and pyrazole moieties confirms interaction of these moieties with the Pb(II) ions. This interaction involves transfer of electronic charge from SP to Pb(II) ions.

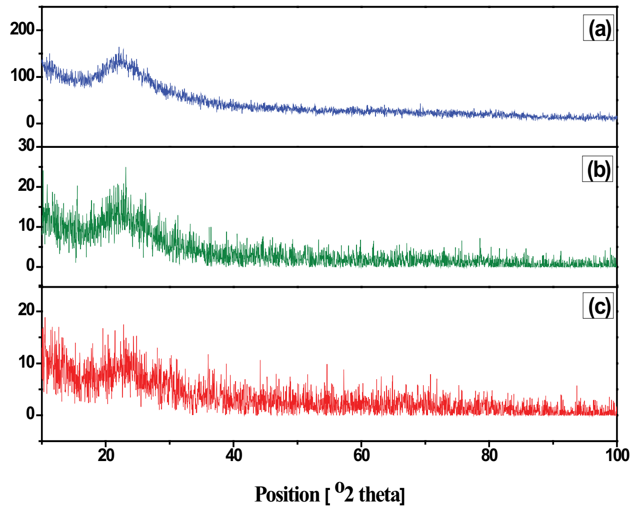

Fig. 6. X-ray diffraction spectra of SG (a), SN (b), SP (c).

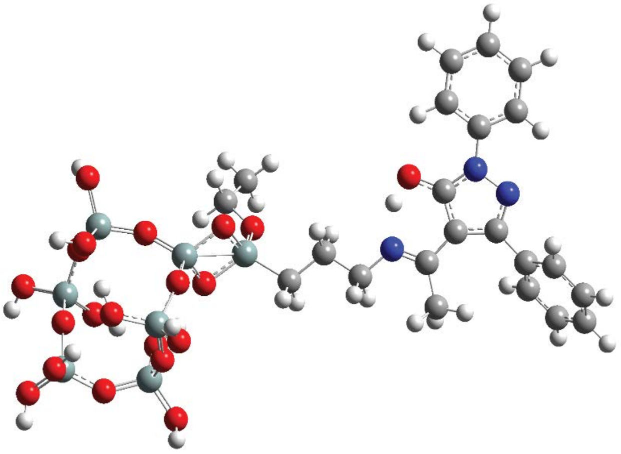

Fig. 7. Optimized geometry of silica supported pyrazole derivative (SP).

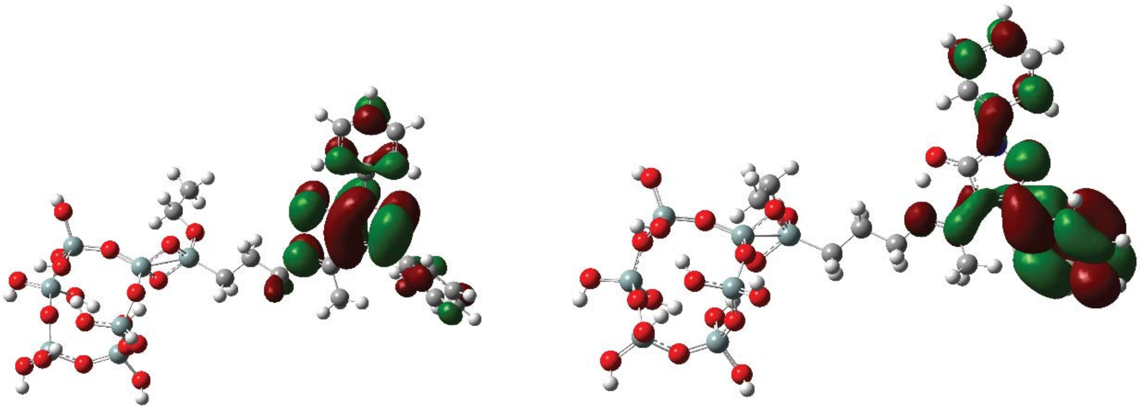

Fig. 8. HOMO (left) and LUMO (right) of silica supported pyrazole derivative (SP).

3.3. Adsorption studies

3.3.1. Optimization of adsorption parameters

The concentration of adsorbent (mass in g or mg) is an important parameter for the process of adsorption. In this research the adsorption capacity (q_e) increased increasing the adsorbent dose from 5 to 30 mg, till a maximum state (20 mg) reached where all binding sites were occupied. Further increasing the adsorbent dose did not show any significant increase in q_e which was consistent to literature [44]. Maximum adsorption capacity (84.16 mg/g) and utmost removal of metal (67.33%) were obtained with optimum dose of 20 mg SP adsorbent.

The effect of pH is a prominent factor in evaluating the suitability and usefulness of the new adsorbent for the metal ions removal. Below pH 5, the ligand is in entirely protonated form, thus forming a positively charged monolayer on surface of silica. Increasing the pH, weakens the protonation and therefore improves metal ion chelation and adsorption capacity. For pH > 8, concentration of metal ion decreases as a result of hydrolysis of metal ion making it difficult to distinguish between adsorbed and hydrolyzed metal ions [44,45].The pH range of 5–7 was investigated for Pb(II) metal ion removal by SP and a significant change in the adsorption capacity was observed, as shown in Fig. 9. Maximum removal of lead ions Pb(II) (95.33%) and highest adsorption capacity (119.16 mg/g) was observed at pH of 6.8 i.e. optimum pH for this adsorbent.

The process of adsorption covers in two steps: in the former step, adsorption capacity increases rapidly because of high availability of active binding sites at the start, however in the later step, q_t changes very slowly as active sites are saturated [46]. Therefore, in order to find required minimum time to attain maximum adsorption efficiency of adsorbent for metal ion removal, the effect of stirring time was optimized from 0 to 120 min. The optimum time for maximum adsorption (120.833 mg/g) to take place was 30 min with 96.66% removal of metal.

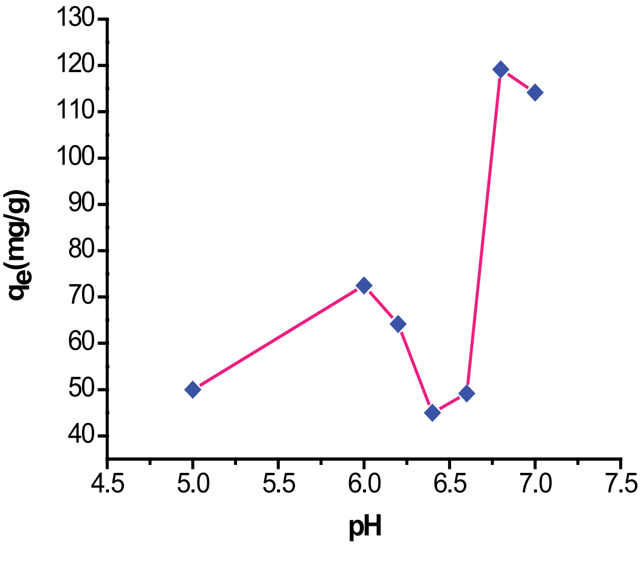

Fig. 9. Effect of pH on eradication of Pb(II) by adsorbent (SP).

To determine the temperature effecton the adsorption of Pb(II) by adsorbent SP, a temperature range of 20ºC–50ºC was studied. It was noted that highest adsorption capacity (q_e 118.33 mg/g) and maximum removal of metal (94.66%) occurred at room temperature i.e. 20ºC. Further increase in the temperature decreased the adsorption capacity.

3.3.2. Kinetic modeling

The efficiency of adsorption depends on kinetics of adsorbents. The rapid adsorption time for ca. 30 min indicates that active donor atoms (nitrogen and oxygen) attached to the silica are well-oriented and can easily be accessible for metal ions in the solution. In addition, the donor atoms (nitrogen and oxygen) act as a bidentate convergent chelating donor as they are attached to the same metal atom and form more stable six-membered ring.

The linear form of Lagergren's pseudo first order kinetics and Ho's pseudo second order model can be written as follows:

$$\ln\left(q_e - q_t\right) = \ln q_e - k_1 t \tag{3}$$

$$\frac{t}{q_t} = \frac{1}{k_2 q_e^2} + \frac{t}{q_e} \tag{4}$$

where q_e and q_t are the adsorption capacities (mg g^{-1}) at equilibrium and at time t, and k_1 (min^{-1}) and k_2 (g mg^{-1} min^{-1}) are the rate constant of the first-order adsorption and the second-order adsorption respectively. The graphs for linear pseudo-first order model and linear pseudo-second order model are shown in Figs. 10(a) and (b), respectively. The linear of Weber-Morris's intra-particular diffusion model can be written as follows:

$$q_t = k_{\mathrm{IPD}}\sqrt{t} + C \tag{5}$$

A straight line graph was obtained between q_t and $\sqrt{t}$, with K_{IPD} as slope and C as intercept (Fig. 10(c)).

The results of kinetic models applied are shown in Table 2. High value of determination coefficient ($R^2 = 0.999$) for pseudo-second-order and low values of regression correlation coefficient R^2 for intraparticle diffusion model and pseudo-first-order indicated that pseudo-second-order was being followed in the adsorption of Pb(II) by SP and consistent to literature [42] earlier for similar hybrids. The straight line curve of intraparticle diffusion model did not pass through the origin; which ensured that the process was controlled by more than one mechanism and intra-particle diffusion was not the only rate limiting step. Moreover, the calculated adsorption capacity ($q_{e(\mathrm{cal})}$) for pseudo-second-order model was close enough to the experimental ($q_{e(\mathrm{exp})}$), which also confirmed the validity of this model.

3.3.3. Equilibrium modeling

The initial metal ion concentration (C_o) was varied from 40–60 mg/L at optimized conditions of SP to obtain three different adsorption isotherms. A direct relation between

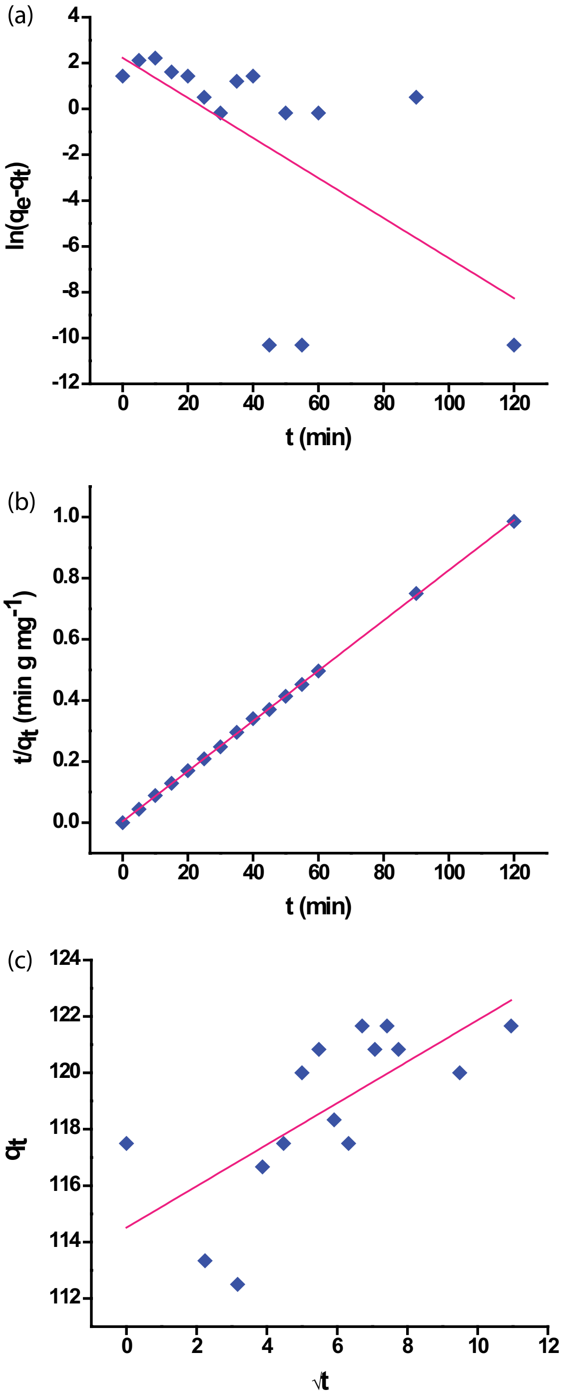

Fig. 10. (a) Pseudo-first-order model for adsorbent (SP), (b) pseudo-second-order model for adsorbent (SP), (c) intraparticle diffusion model for adsorbent (SP).

initial metal ion concentration (C_o) and adsorption capacity (q_e) existed which showed that if the metal ion concentration increases, thenthe adsorption capacitywill also increase.

Three common and important isotherm equations, Langmuir isotherms (based on monolayer adsorption on homogeneous surface), Freundlich isotherms (describes multilayer adsorption on heterogeneous surface) and Dubinin–Radushkevich isotherms (to calculate the mean free energy (E) of adsorption in kJ/mol) were used to evaluate the adsorption. Linear forms of these models can be expressed as follows respectively:

$$\frac{C_e}{q_e} = \frac{C_e}{q_{\max}} + \frac{1}{K_L \times q_{\max}} \tag{6}$$

$$\ln q_e = \ln K_F + \frac{1}{n} \ln C_e \tag{7}$$

$$\ln q_e = \ln q_{\mathrm{DR}} - \beta \in^2 \tag{8}$$

where q_e (mg/g) is the amount of metal sorbed at equilibrium, $q_{\max}$ (mg/g) is the monolayer sorption capacity, K_L (L/mg) is the Langmuir constant, C_e (mg/L) is the concentration of metal ion solution at equilibrium, $1/n$ is the heterogeneity factor, K_F (L/mg) is the Freundlich constant, q_{DR} is the D-R constant, $\in$ is the Polanyi potential (ε = RT ln(1 + 1/C_e)), R is the general gas constant and T is the absolute temperature. Data of these models are represented in Table 3.

The regression correlation value ($R^2 = 0.968$) for Langmuir model (Fig. 11) was close to ideal value, indicated the validity of this model. The value of adsorption capacity calculated by Langmuir model ($q_{\max} =$ 142.8571 mg/g) was close enough to that of experimental value ($q_e =$ 120.833 mg/g). A dimensionless separation factor (R_L) explains the shape and feasibility of Langmuir isotherm which is calculated as follows:

$$R_L = \frac{1}{1 + K_L C_o} \tag{9}$$

The adsorption is irreversible if R_L is 0. The process is unfavorable if $R_L > 1$. The process is only favorable if R_L is $0 < R_L < 1$. The value of R_L for adsorbent SP (0.00474-0.00709) also ensured the validity of Langmuir model.

The low values of R^2 for Freundlich ($R^2 = 0.739$) and D-R ($R^2 = 0.681$) suggested that these models were less fitted in this case. The value of n from Freundlich model indicates the favorability of the reaction. If $n = 1$, linear adsorption occurs. If $n > 1$ then reaction takes place favorably as in the case for adsorbent SP ($n = 8.928571$) was observed. The mean free energy (($E = 1/\sqrt{2\beta}$) kJ/mol) tells about the physical ($E <$ 8kJ/mol) or chemical (E is 8–16 kJ/mol) nature of adsorption.

Table 2
Kinetic modeling for eradication of Pb(II) by SP

Pseudo-first-order			Pseudo-second-order			Intraparticle diffusion	
q_e (mg/g)	k_1 (1/min)	R^2	q_e (mg/g)	k_2 (g/mg/min)	R^2	k_{IPD} (mg/g/min)	R^2
9.28128	–0.087	0.357	125	0.016	0.999	0.736	0.493

Table 3
Adsorption isotherms and their parameters for adsorbent SP

Model	Parameter	Pb(II)
Langmuir	$q_{\max}$(mg/g)	142.8571
	K_L(L/mg)	3.500001
	R^2	0.968
	R_L	0.00474–0.00709
Freundlich	K_F(mg/g)	102.1048
	N	8.928571
	R^2	0.739
D-R	q_{DR}(mg/g)	124.2133
	β (mol²/J²)	5 × 10^{-8}
	E (kJ/mol)	3.162278
	R^2	0.681

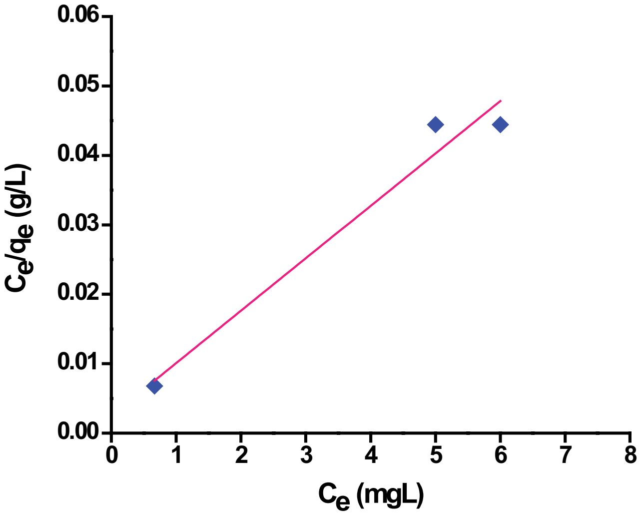

Fig. 11. Langmuir adsorption model fit for eradication of Pb(II) by adsorbent (SP).

For the adsorption of Pb(II) by adsorbent SP, E was less than 8 kJ/mol indicated physical [44] nature of adsorption but low value of R^2 suggested that adsorption process was not governed by this model.

On comparing three isotherms, the parameters of Langmuir model (R^2, $q_{\max}$ and R_L) ensured that it was the best fit model for the adsorption of Pb(II) metal ions by SP adsorbentaand also consistent to the literature [42]. This indicated that there was a saturated monolayer of Pb^{2+} ions upon the homogenous surface of adsorbent SP related to the maximum adsorption and no mutual interactions between the sorbed Pb(II) ions was present.

3.3.4. Thermodynamic studies

For the evaluation of temperature effect on the eradication of Pb(II) by SP, the temperature was varied from 30°C to 50°C. A graph was plotted between T_K and $\Delta G°$ (Fig. 12) and following thermodynamic equations were used to determine the equilibrium constant K_D value, thermodynamic parameters, Gibbs free energy change ($\Delta G°$), entropy change ($\Delta S°$) and enthalpy change ($\Delta H°$):

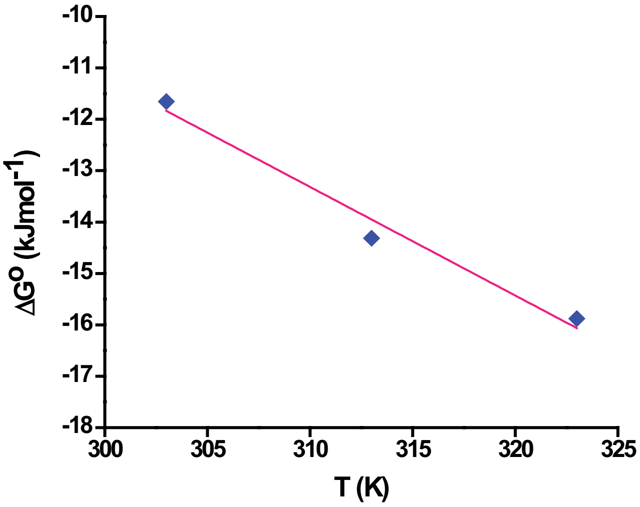

Fig. 12. Thermodynamic study for the eradication of Pb(II) by SP at optimum conditions.

$$\ln K_D = \frac{\Delta S}{R} - \frac{\Delta H}{RT} \tag{10}$$

$$\Delta G° = \Delta H° - T\Delta S° \tag{11}$$

$$K_D = \frac{\left(C_o - C_e\right)V}{C_e m} \tag{12}$$

where C_o (mg/L) is the initial concentration of metal ion, C_e (mg/L) is the equilibrium metal ion concentration, m (g) is the mass of adsorbent and V (L) is the volume of the metal solution, T (K) is the absolute temperature and R (8.314 J/mol/K) being general gas constant.

Thermodynamic parameters are shown in Table 4. The Gibb's free energy ($\Delta G°$) gave negative values for all the temperature range indicating the spontaneous nature of adsorption. The positive $\Delta H°$ value revealed the endothermic nature of adsorption and its value ($\Delta H° > 40$ kJ/mol) confirmed chemical adsorption; however the positive $\Delta S°$ indicated the increase in randomness of the adsorption.

3.3.5. Comparison with the literature

Our novel synthesized adsorbent (SP) showed adsorption capacity (q_e) of 120.8333 mg/g with 50 mg/L of Pb(II) solution

Table 4
Thermodynamic parameters for eradication of Pb(II) by SP

T (K)	$\Delta G°$ (kJ/mol)	$\Delta H°$ (kJ/mol)	$\Delta S°$ (J/k/mol)	R^2
303	−11.6549	52.1849	0.2113	0.978
313	−14.3163			
323	−15.8808			

Table 5
Comparison of SP and relevant sorbents for Pb(II) absorption

Ligand (support-silica gel)	q_e (mg/g)	Reference
This work	120.8333	
pyrazol-enol-imine	94.18	[43]
Pyrazol-3-carbaldehyde	74.89	[10]
Gallic acid	12.63	[47]
Ethylediamine derivatives	38.12	[48]
C,N-pyridylpyrazole	09.5	[20]
Thiophene	11.3	[49]
Acid red 88	03.35	[50]
Dithizone	08.28	[51]
Resacetophenone	13.79	[4]
Tris(2-aminoethyl) amine	64.61	[52]

using 20 mg of adsorbent at pH 6.8 and stirring for 30 minutes at room temperature. Comparison of adsorption capacity (q_e) of related adsorbents in literature (Table 5) showed that our novel adsorbent SP revealed much better adsorption capacity than the available adsorbents in literature.

3.3.6. Regenerability of SP

The adsorbent after adsorbing Pb(II) ions can be regenerated easily by shaking it in 5 mL of 6 N HCl for 5 min, washed with water and dried in oven. The adsorption capacity of this regenerated material was 114 mg/g. The adsorbent was regenerated and reused five times but no significant decrease in its adsorption capacity was found. This suggested that no change in the chemical structure of the adsorbent occurred as a result of acid treatment which was confirmed by FTIR. Therefore, this novel material SP proved to be not only efficient adsorbent for Pb(II) ions but also has good chemical stability.

4. Conclusion

A novel chelating agent has been successfully synthesized by immobilizing 1-(1,3-diphenyl-5-hydroxy-1*H*-pyrazol-4-yl)ethanone on 3-aminopropyltrimethoxysilane modified silica gel. The structure of new material was well characterized by FTIR,^{29} Si and ^{13}C solid state NMR, SEM and XRD and Elemental Analysis. The surface area of the material was measured by BET equation. The material has good thermal stability determined by TGA curves. From optimized geometry, FTIR and frontier molecular orbital analysis were carried out. This new chelating agent effectively removed Lead ions Pb(II) from the aqueous solution (120.83 mg of Pb(II)/g of silica gel). All the important parameters for adsorption such as adsorbent concentration, pH, contact time and temperature were studied. The adsorption process fitted into Langmuir isotherm model and followed pseudo-second order kinetics. Thermodynamic parameters revealed that the adsorption process was endothermic (positive $\Delta H°$) and spontaneous in nature (negative $\Delta G°$) with positive value of entropy ($\Delta S°$). Reusability of this adsorbent was checked up to five cycles. Our adsorbent proved a novel, an efficient, a low cost and a reusable adsorbent for Pb(II) ions removal.

Acknowledgements

The authors gratefully acknowledge Higher Education Commission, Pakistan for providing research funds. The authors also acknowledge the laboratory staff and technicians at Institute of Chemistry, University of the Punjab for FTIR and atomic absorption measurements.

Conflicts of Interest

The authors declare that there is no conflict of interest regarding the publication of this paper.

References

[1] S. Babel, T.A. Kurniawan, Low-cost adsorbents for heavy metals uptake from contaminated water: a review, J. Hazard. Mater., 97 (2003) 219–243.

[2] L.R. Bravo-Sánchez, B.S.V. de la Riva, J.M. Costa-Fernández, R. Pereiro, A. Sanz-Medel, Determination of lead and mercury in sea water by preconcentration in a flow injection system followed by atomic absorption spectrometry detection, Talanta, 55 (2001) 1071–1078.

[3] M.M. Saeed, M. Ahmed, Retention, kinetics and thermodynamics profile of cadmium adsorption from iodide medium onto polyurethane foam and its separation from zinc bulk, Anal. Chim. Acta, 525 (2004) 289–297.

[4] A. Goswami, A.K. Singh, Silica gel functionalized with resacetophenone: synthesis of a new chelating matrix and its application as metal ion collector for their flame atomic absorption spectrometric determination, Anal. Chim. Acta, 454 (2002) 229–240.

[5] J. Judkins Jr, J.S. Hornsby, Color removal from textile dye waste using magnesium carbonate, J. Water Pollut. Control Fed., 50 (1978) 2446–2456.

[6] C. Namasivayam, S. Senthilkumar, Removal of arsenic (V) from aqueous solution using industrial solid waste: adsorption rates and equilibrium studies, Ind. Eng. Chem. Res., 37 (1998) 4816–4822.

[7] A. Sarkar, P. Datta, M. Sarkar, Sorption recovery of metal ions using silica gel modified with salicylaldoxime, Talanta, 43 (1996) 1857–1862.

[8] P.M. Price, J.H. Clark, D.J. Macquarrie, Modified silicas for clean technology, J. Chem. Soc., Dalton Trans., (2000) 101–110.

[9] S. Radi, A. Attayibat, A. Ramdani, M. Bacquet, Synthesis and characterization of novel porous SiO_2 material functionalized with C, C-pyridylpyrazole receptor, J. Appl. Polym. Sci., 117 (2010) 3345–3349.

[10] S. Radi, S. Tighadouini, M. Bacquet, S. Degoutin, F. Cazier, M. Zaghrioui, Y.N. Mabkhot, Organically modified silica with pyrazole-3-carbaldehyde as a new sorbent for solid-liquid extraction of heavy metals, Molecules, 19 (2013) 247–262.

[11] C. Yélamos, M.J. Heeg, C.H. Winter, Synthesis, structure, and reactivity of potassium pyrazolato complexes: the first structurally documented η2-pyrazolato coordination by a main group metal, Inorg. Chem., 37 (1998) 3892–3894.

[12] D. Pfeiffer, M.J. Heeg, C.H. Winter, Magnesium complexes bearing η2-pyrazolato ligands, Angew. Chem. Int. Ed., 37 (1998) 2517–2519.

[13] R. Mathieu, G. Esquius, N. Lugan, J. Pons, J. Ros, Bis [(3, 5-dimethyl-1-pyrazolyl) methyl] ethylamine– a versatile ligand for complexation in RhI cationic complexes, Eur. J. Inorg. Chem., 2001 (2001) 2683–2688.

[14] S. Trofimenko, Recent advances in poly (pyrazolyl) borate (scorpionate) chemistry, Chem. Rev. (Washington, DC, U.S.), 93 (1993) 943–980.

[15] S. Trofimenko, Progress in Inorganic Chemistry, vol. 34, Wiley-Interscience, New York, 1986.

[16] G. Ma, H. Freiser, S. Muralidharan, Centrifugal partition chromatographic separation of tervalent lanthanides using acylpyrazolone extractants, Anal. Chem., 69 (1997) 2835–2841.

[17] S. Radi, A. Attayibat, M. El-Massaoudi, M. Bacquet, S. Jodeh, I. Warad, S.S. Al-Showiman, Y.N. Mabkhot, C, N-bipyrazole receptor grafted onto a porous silica surface as a novel adsorbent based polymer hybrid, Talanta, 143 (2015) 1–6.

[18] S. Tighadouini, S. Radi, A new silica hybrid material based adsorbent with NCC-bipyrazolic tripodal receptor for environmental purpose, Arab. J. Chem. Environ. Res., 2 (2015) 1–14.

[19] S. Radi, S. Tighadouini, Y. Toubi, M. Bacquet, Polysiloxane surface modified with bipyrazolic tripodal receptor for quantitative lead adsorption, J. Hazard. Mater., 185 (2011) 494–501.

[20] S. Radi, A. Ramdani, Y. Lekchiri, M. Morcellet, G. Crini, L. Janus, M. Bacquet, Immobilization of pyrazole compounds on silica gels and their preliminary use in metal ion extraction, New J. Chem., 27 (2003) 1224–1227.

[21] O. Todorova, P. Vassileva, L. Lakov, Synthesis and characterization of inorganic sorbents containing pyrazolone, Fresenius J. Anal. Chem., 346 (1993) 943–946.

[22] S. Radi, A. Attayibat, A. Ramdani, M. Bacquet, Synthesis and characterization of novel silica gel supported N-pyrazole ligand for selective elimination of Hg (II), Eur. Polym. J., 44 (2008) 3163–3168.

[23] P. Verweij, M. Haanepen, J. De Ridder, W. Driessen, J. Reedijk, Synthesis, characterization and metal-uptake behaviour of pyrazole ligands immobilized on silica, Recl. Trav. Chim. Pays-Bas, 111 (1992) 371–378.

[24] S. Radi, A. Ramdani, Y. Lekchiri, M. Morcellet, G. Crini, L. Janus, B. Martel, Extraction of metal ions from water with tetrapyrazolic macrocycles bound to Merrifield resin and silica gel, J. Appl. Polym. Sci., 78 (2000) 2495–2499.

[25] A.S. Amarasekara, O.S. Owereh, S.K. Aghara, Synthesis of 4-acylpyrazolone Schiff base ligand grafted silica and selectivity in adsorption of lanthanides from aqueous solutions, J. Rare Earths, 27 (2009) 870–874.

[26] C. Lin, H. Wang, Y. Wang, Z. Cheng, Selective solid-phase extraction of trace thorium (IV) using surface-grafted Th (IV)-imprinted polymers with pyrazole derivative, Talanta, 81 (2010) 30–36.

[27] N. Jiang, X. Chang, H. Zheng, Q. He, Z. Hu, Selective solid-phase extraction of nickel (II) using a surface-imprinted silica gel sorbent, Anal. Chim. Acta, 577 (2006) 225–231.

[28] E. Melek, M. Tuzen, M. Soylak, Flame atomic absorption spectrometric determination of cadmium (II) and lead (II) after their solid phase extraction as dibenzyldithiocarbamate chelates on Dowex Optipore V-493, Anal. Chim. Acta, 578 (2006) 213–219.

[29] T. Duan, X. Song, D. Jin, H. Li, J. Xu, H. Chen, Preliminary results on the determination of ultratrace amounts of cadmium in tea samples using a flow injection on-line solid phase extraction separation and preconcentration technique to couple with a sequential injection hydride generation atomic fluorescence spectrometry, Talanta, 67 (2005) 968–974.

[30] K. Suvardhan, K.S. Kumar, D. Rekha, B. Jayaraj, G.K. Naidu, P. Chiranjeevi, RETRACTED: Preconcentration and solid-phase extraction of beryllium, lead, nickel, and bismuth from various water samples using 2-propylpiperidine-1-carbodithioate with flame atomic absorption spectrometry (FAAS), Talanta, 68 (2006) 735–740.

[31] J. Fang, Y. Jiang, X.-P. Yan, Z.-M. Ni, Selective quantification of trace palladium in road dusts and roadside soils by displacement solid-phase extraction online coupled with electrothermal atomic absorption spectrometry, Environ. Sci. Technol., 39 (2005) 288–292.

[32] A.-M. Putz, A. Len, C. Ianăşi, C. Savii, L. Almásy, Ultrasonic preparation of mesoporous silica using pyridinium ionic liquid, Korean J. Chem. Eng., 33 (2016) 749–754.

[33] J. Haginaka, Selectivity of affinity media in solid-phase extraction of analytes, TrAC, Trends Anal. Chem., 24 (2005) 407–415.

[34] F. Marchetti, C. Pettinari, A. Cingolani, R. Pettinari, M. Rossi, F. Caruso, Organotin (IV) derivatives of novel β-diketones: part V. Synthesis and characterization of di-and triorganotin (IV) derivatives of 4-acyl-5-pyrazolones modified in position 3 of the pyrazole. Crystal structure of (1, 3-diphenyl-4-benzoyl-pyrazolon-5-ato) triphenyltin (IV), J. Organomet. Chem., 645 (2002) 134–145.

[35] B.S. Jensen, The synthesis of 1-phenyl-3-methyl-4-acyl-pyrazolones-5, Acta Chem. Scand, 13 (1959) 1668–1670.

[36] M.J. Frisch, H.B. Schlegel, G.E. Scuseria, J.R.M.A. Robb, V.G.Z. Cheeseman, J.J.A. Montgomery, R.E. Stratmann, J.C. Burant, J.M.M.S. Dapprich, K.N.K.A.D. Daniels, M.C. Strain, J.O. Farkas, V.B. Tomasi, M. Cossi, R. Cammi, B. Mennucci, Gaussian 09, Rev C.01., Wallingford, Pittsburg, CT, 2010.

[37] D.-M. Han, G.-Z. Fang, X.-P. Yan, Preparation and evaluation of a molecularly imprinted sol–gel material for on-line solid-phase extraction coupled with high performance liquid chromatography for the determination of trace pentachlorophenol in water samples, J. Chromatogr., A, 1100 (2005) 131–136.

[38] Y. Jiang, Q. Gao, H. Yu, Y. Chen, F. Deng, Intensively competitive adsorption for heavy metal ions by PAMAM-SBA-15 and EDTA-PAMAM-SBA-15 inorganic–organic hybrid materials, Microporous Mesoporous Mater., 103 (2007) 316–324.

[39] S. Ek, E.I. Iiskola, L. Niinistö, J. Vaittinen, T.T. Pakkanen, A. Root, A ^{29}Si and ^{13}C CP/MAS NMR study on the surface species of gas-phase-deposited γ-aminopropylalkoxysilanes on heat-treated silica, J. Phys. Chem. B, 108 (2004) 11454–11463.

[40] W. Lutz, D. Täschner, R. Kurzhals, D. Heidemann, C. Hübert, Characterization of silica gels by ^{29}Si MAS NMR and IR spectroscopic measurements, Zeitschrift für anorganische und allgemeine Chemie, 635 (2009) 2191–2196.

[41] J.A. Sales, F.P. Faria, A.G. Prado, C. Airoldi, Attachment of 2-aminomethylpyridine molecule onto grafted silica gel surface and its ability in chelating cations, Polyhedron, 23 (2004) 719–725.

[42] S. Radi, S. Tighadouini, M. Bacquet, S. Degoutin, B. Revel, M. Zaghrioui, Quantitative removal of Zn (II) from aqueous solution and natural water using new silica-immobilized ketoenol–pyridine receptor, J. Environ. Chem. Eng., 3 (2015) 1769–1778.

[43] S. Tighadouini, S. Radi, M. Bacquet, S. Degoutin, M. Zaghrioui, S. Jodeh, I. Warad, Removal efficiency of Pb (II), Zn (II), Cd (II) and Cu (II) from aqueous solution and natural water by ketoenol–pyrazole receptor functionalized silica hybrid adsorbent, Sep. Sci. Technol., 52 (2017) 608–621.

[44] F. Farooq, U. Farooq, M. Batool, M. Athar, M. Salman, Q. Ahmed, A. Ashraf, Use of wheat straw for effective binding of metal ions via a novel modification, Korean J. Chem. Eng., 32 (2015) 1818–1826.

[45] M.K. Mondal, Removal of Pb (II) from aqueous solution by adsorption using activated tea waste, Korean J. Chem. Eng., 27 (2010) 144–151.

[46] J. Lehn, J. Sauvage, Cryptates. XVI.[2]-Cryptates. Stability and selectivity of alkali and alkaline-earth macrobicyclic complexes, J. Am. Chem. Soc., 97 (1975) 6700–6707.

[47] F. Xie, X. Lin, X. Wu, Z. Xie, Solid phase extraction of lead (II), copper (II), cadmium (II) and nickel (II) using gallic acid-modified silica gel prior to determination by flame atomic absorption spectrometry, Talanta, 74 (2008) 836–843.

[48] N. Chiron, R. Guilet, E. Deydier, Adsorption of Cu (II) and Pb (II) onto a grafted silica: isotherms and kinetic models, Water Res., 37 (2003) 3079–3086.

[49] S. Radi, A. Attayibat, Functionalized SiO_2 with S-donor thiophene: synthesis, characterization, and its heavy metals adsorption, Phosphorus Sulfur Silicon, 185 (2010) 2003–2013.

[50] R. Kocjan, Retention of some metal ions and their separation on silica gel modified with Acid Red 88, Microchim. Acta, 131 (1999) 153–158.

[51] O. Zaporozhets, N. Petruniock, V. Sukhan, Determination of Ag (I), Hg (II) and Pb (II) by using silica gel loaded with dithizone and zinc dithizonate, Talanta, 50 (1999) 865–873.

[52] X. Huang, X. Chang, Q. He, Y. Cui, Y. Zhai, N. Jiang, Tris (2-aminoethyl) amine functionalized silica gel for solid-phase extraction and preconcentration of Cr (III), Cd (II) and Pb (II) from waters, J. Hazard. Mater., 157 (2008) 154–160.

Supplementary Information

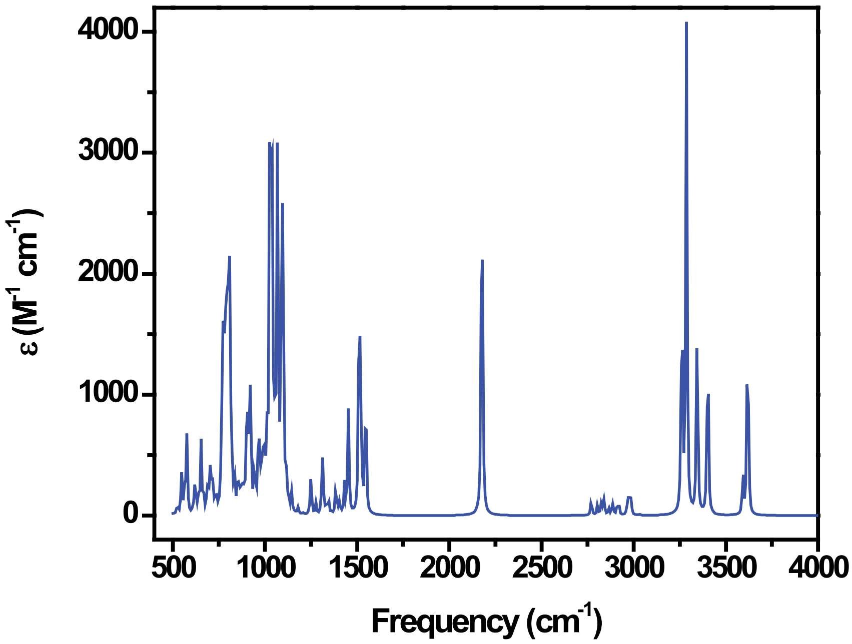

Fig. S1. Theoretically calculated FTIR spectrum of SP.